Kinetic Monte Carlo simulation of dislocation dynamics

Karin Lin
Department of Physics, University of California, Berkeley, California 94720
and Division of Materials Sciences, Lawrence Berkeley National Laboratories, Berkeley, California 94720

D. C. Chrzan
Division of Materials Sciences, Lawrence Berkeley National Laboratories, Berkeley, California 94720
and Department of Materials Science and Mineral Engineering, University of California, Berkeley, California 94720
(Received 26 January 1999)

A kinetic Monte Carlo simulation of dislocation motion is introduced. The dislocations are assumed to be composed of pure edge and screw segments confined to a fixed lattice. The stress and temperature dependence of the dislocation velocity is studied, and finite-size effects are discussed. It is argued that surfaces and boundaries may play a significant role in the velocity of dislocations. The simulated dislocations are shown to display kinetic roughening according to the exponents predicted by the Kardar-Parisi-Zhang equation. [S0163-1829(99)11429-2]

I. INTRODUCTION

The *a priori* prediction of mechanical properties remains an outstanding problem in materials physics. At the current time, it appears that the only viable means to address this problem is through the use of ''multiscale modeling.''[1] In this approach, one attempts to calculate properties of dislocation cores and short ranged dislocation-dislocation interactions using atomic scale techniques. The results of these calculations are then incorporated into larger scale simulations of dislocation dynamics. Typically, the dynamics of the individual dislocations are treated within a simple approximation based on a mean-field approach.[2,3] However, at high stresses and temperatures, it is no longer clear whether the mean-field formulation is appropriate. Ascertaining the relevance of the mean-field solution to more extreme conditions is an important endeavor, particularly if one wishes to make *quantitative* predictions for mechanical behavior.

The purpose of the current paper, then, is to explore the dynamics of a single dislocation bounded by free surfaces moving through a Peierls barrier through kink nucleation and motion. Specifically, the stress and temperature dependence of a simplified dislocation moving through a deep Peierls potential (both primary and secondary) is studied using kinetic Monte Carlo simulations. The model, while simple, reflects the long ranged elastic interactions of the kinks and hence allows one to estimate the importance of these interactions towards determining the dislocation velocity. The elastic effects of the surface are incorporated explicitly, and this allows one to discern the importance of the boundaries in determining dislocation velocities. Further, the simulations allow one to discern which atomic scale processes are most important for determining the velocity of a dislocation, and hence may serve as a guide to smaller scale calculations.

Through simulation and subsequent modeling, it is established here that (1) Surfaces and boundaries may alter the dislocation velocity substantially. (2) The effect of temperature on the dislocation velocity is a function of the applied stress; thermal fluctuations accelerate dislocation motion at low stresses and may ''retard'' the dislocation motion at high stresses. (3) Dislocations may display kinetic roughening. The roughening is described by the exponents expected from the analogous crystal growth problem.

The remainder of this paper is organized as follows. In the next section, the model is described. Section III presents an analysis of the effects of finite size on the average velocity of the dislocation. Section IV presents the analysis which reveals the kinetic roughening of the simulated dislocations, and Sec. V presents the conclusions.

II. DISLOCATION MODEL

A. Representation of the dislocation

The dislocation is modeled as a system of pure screw and pure edge segments on a two-dimensional (2D) rectangular lattice. Screw segments are assumed to lie in Peierls minima. The lattice is infinite in the direction of motion and bounded by free surfaces in the direction perpendicular to motion (see Fig. 1). The dislocation moves under the influence of thermal fluctuations and an optional applied stress, via the processes of double-kink nucleation and lateral kink motion. Length parameters are chosen to be consistent with a (110) slip plane of tantalum. The discretization distance in the direction of motion is simply the distance between neighboring Peierls valleys $a=(2/3)^{1/2}a_0=2.14$ Å, where $a_0=3.03$ Å is the

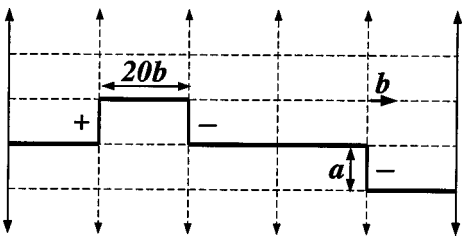

FIG. 1. Discrete model of a dislocation. Screw segments lie in Peierls minima and edge segments are present only as kinks. The + and − signs indicate positive and negative kinks, respectively.

lattice constant. The discretization distance in the direction perpendicular to motion is chosen to be $20b$, where b is the Burgers vector equal to $a\sqrt{3}/2=2.6$ Å. It is found that kink pairs separated by the minimum distance of b are unstable at normal stresses and temperatures, and that the Peierls barrier is nearly always insignificant compared to the energy associated with the elastic deformation of the dislocation. The kink pair separation distance is thus *chosen* to be $20b$, which gives stable kink pairs at most stresses and temperatures and improves computational efficiency by reducing the number of nucleation and kink motion events for a dislocation of a given length.

It is known that the kink pair nucleation distance is variable, and that the equilibrium distance is stress dependent.[2,4] However, incorporating these facts into a Monte Carlo simulation is nontrivial. In particular, maintaining detailed balance in the presence of a variable nucleation width is difficult, and failure to maintain detailed balance can lead to serious artifacts in the dislocation's structure. Therefore, the present treatment chooses to maintain detailed balance while sacrificing other physical detail.

B. Dislocation evolution

The initial state of the dislocation is a perfectly straight, single screw-oriented segment. Evolution of the dislocation is controlled by standard kinetic Monte Carlo procedure[5] as follows. At each stage of the simulation, all allowed events are calculated. These include double-kink nucleation, annihilation of an existing kink pair, and lateral motion of a single kink. Both events that move the dislocation in the direction favored by the stress and events that move it against the stress are allowed, since thermal fluctuations can overcome the additional energy bias caused by the stress. Each event is then assigned a rate according to

$$R=\omega_0 \exp(-\Delta E_{\mathrm{barr}}/k_B T) \tag{1}$$

where ω_0 is an attempt frequency and ΔE_{barr} is the energy barrier associated with moving between the initial and final configurations. The sum of all the rates is then used to determine the time before the next event occurs, and the individual rates serve as probabilities for selecting the event.

For double-kink nucleation and annihilation, ΔE_{barr} in Eq. (1) is determined by comparing the energies

$$\Delta E_{\mathrm{mid}}=\Delta E_s(a/2)+\Delta E_P, \tag{2}$$

$$\Delta E_{\mathrm{final}}=\Delta E_s(a), \tag{3}$$

where ΔE_P is the Peierls energy and

$$\Delta E_s(y)=\Delta E_{s,\mathrm{elastic}}(y)\pm\sigma b(20b)y \tag{4}$$

includes the elastic energy required to move a screw segment a distance y and the work done by or against the applied stress. Once ΔE_{mid} and $\Delta E_{\mathrm{final}}$ are calculated,

$$\Delta E_{\mathrm{barr}}=\begin{cases}\Delta E_{\mathrm{mid}} & \Delta E_{\mathrm{mid}}\geqslant\Delta E_{\mathrm{final}} \quad \text{and} \quad \Delta E_{\mathrm{mid}}>0,\\ \Delta E_{\mathrm{final}}/2 & \text{otherwise}.\end{cases} \tag{5}$$

One might naturally expect ΔE_{barr} always to be defined by ΔE_{mid}, since the Peierls potential has a maximum at the halfway point. However, the Peierls energy is not always the dominating factor in the energy barrier. In some cases, the elastic energy required to move a screw segment to its final position exceeds that required to move it to the halfway position by an amount greater than the Peierls energy. Also, when the applied stress is large, double-kink nucleation is so favorable that the energy barrier is negative, and the screw segment will move immediately to its final position. An ideal calculation would take into account the analytical forms of the three contributions to the energy barrier—the elastic energy, Peierls energy, and work due to applied stress—as continuous functions of the screw segment position, and calculate the maximum barrier exactly. However, the complexity of the elastic energy calculation, as well as its dependence on the entire dislocation configuration, makes such a calculation computationally unfeasible. This scheme, in which the energy barriers for only the halfway position and final position are calculated, allows for a more accurate choice of ΔE_{barr} without sacrificing computational efficiency. The factor of 2 must be added to $\Delta E_{\mathrm{final}}$ to ensure that detailed balance is obeyed.

For lateral kink motion,

$$\Delta E_{\mathrm{barr}}=\Delta E_e(20b)/2+\Delta_{\mathrm{mig}}, \tag{6}$$

where Δ_{mig} is a kink migration energy and

$$\Delta E_e(x)=\Delta E_{e,\mathrm{elastic}}(x)\pm\sigma bax \tag{7}$$

includes the elastic energy required to move an edge segment a distance x and the work done by or against the applied stress. Again, the factor of 2 is added to ensure that detailed balance is obeyed.

The parameters ω_0 and ΔE_P are determined as follows. The attempt frequency ω_0 is chosen to be the fundamental mode of the Granato-Lücke vibrating string model[2]

$$\omega_0=C_t\pi/L \tag{8}$$

using the double-kink separation length $L=20b$ and speed of sound in tantalum $C_t=2060$ m/s, which gives $\omega_0=1.23\times10^{12}$. This *estimate* sets the overall scale for the velocity; there is no *a priori* reason to expect double kink nucleation, and kink migration to be governed by the same attempt frequency. The current treatment, however, makes this assumption, and its significance remains to be tested. Experimental measurements and theoretical estimates of the Peierls stress in tantalum cover a wide range, from 340–1100 MPa.[6–8] For these simulations, σ_P was chosen to be 750 MPa, corresponding to $\Delta E_P=0.44$ eV for a screw segment of length $20b$.

The calculations of $\Delta E_{s,\mathrm{elastic}}(y)$ and $\Delta E_{e,\mathrm{elastic}}(x)$ are the most computationally intensive part of the simulation. Each calculation is performed within isotropic elasticity theory[2] and includes all segment-segment interactions. To minimize surface effects, nucleation, and annihilation of single kinks are allowed to occur at a distance of $10b$ from the surface. Image stresses and surface traction terms[9,10] are included in the calculation; properly, this requires an infinite sum over all reflections of the images on both surfaces. However, the interactions drop off rapidly as functions of both the distance from the surface of the stress-generating segment and the distance between the segment and the point of evaluation,

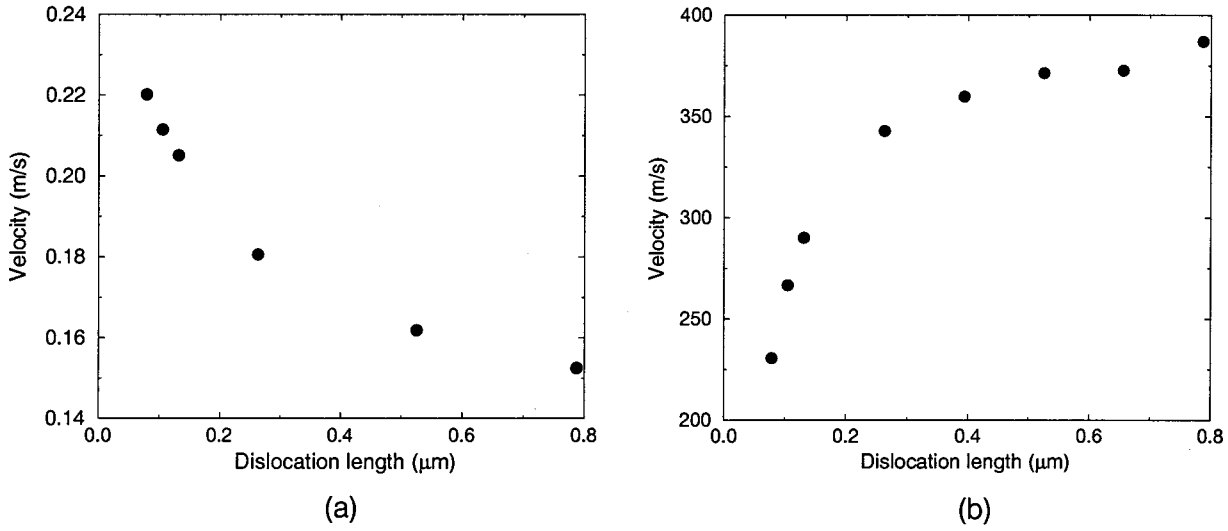

FIG. 2. Dislocation velocity vs length for an applied stress of (a) 100 MPa and (b) 400 MPa at a sample temperature of 450 K.

and are significant only for segments very near the surface. Thus, only the first term in the sum is included for each segment with each surface.

The additional energetic barrier to lateral kink motion Δ_{mig}, which may be thought of as a secondary Peierls barrier, warrants further discussion. The direct connection between this barrier and the microscopic kink migration process is not clear. Atomic scale calculations are necessary to reveal the dynamics governing kink motion over distances of the order of b.[11–14] In addition, since ''real'' kinks move through barriers with a periodicity of b, there should be an entropic contribution to the rate at which model kinks move a distance of $20b$. The kink barrier is a construct which allows tuning of the relative rates of kink motion and double kink nucleation or annihilation, and the value $\Delta_{\mathrm{mig}} = 0.25$ eV is chosen so that the rates of these two types of events are comparable. The experimental observation of dislocations with low kink mobility[8,15] suggest that this choice is not unreasonable.

III. DISLOCATION VELOCITY

A. Finite-size effects

Because the computational demands of the simulation place a limit on the dislocation length that can be considered, it is crucial to examine the effects of finite size, particularly with regard to the presence of the free surfaces that bound the dislocation. Further, dislocations in nature are often bounded by surfaces or interfaces. These defects may influence the dislocation velocities. In order to study the dependence of the steady-state dislocation velocity on dislocation length, a simpler model is used in which only two elastic energies are calculated, that associated with nucleating a kink pair and that associated with moving a single kink in the middle of an otherwise flat dislocation. These two quantities are then taken to be the elastic contribution to the energies used in computing rates of kink pair nucleation or annihilation and kink pair motion. This simplified description reproduces trends in the statistically steady-state dislocation velocities calculated from the full simulation while allowing the examination of longer dislocation lengths. (The simple model does not, however, accurately reproduce the structure of the dislocation as deduced from examination of the dislocation widths, and thus is used only for the purpose of examining dislocation velocity.)

Figure 2 shows the steady state dislocation velocity as a function of dislocation length for two applied stresses. It is noted that the absolute values of the velocities depend on the choice of the attempt frequency ω_0 and are not meant to be compared to experimental values; rather, they are shown to illustrate qualitatively the different regimes of length dependence.

The dependence of the dislocation velocity on length is a result of two different surface effects, and the nature of the dependence (i.e., whether velocity increases or decreases with length) is determined by the dominance of one effect over the other in different regions of parameter space. On one hand, surfaces can be thought of as kink sources, for they serve to enhance the velocity in the following manner: A kink pair is most likely to ''stick'' when it is nucleated close to the surface, after which the adjacent single-kink annihilation (with its image) is energetically favored, leaving the remaining kink to move laterally within the dislocation (see Fig. 3.) Thus, nucleation of a kink pair near a surface is favored over nucleation in the bulk. On the other hand, sur-

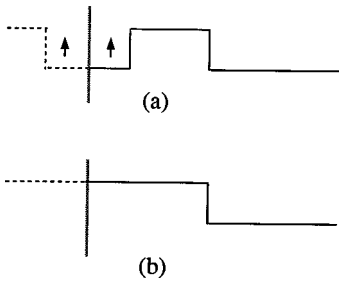

FIG. 3. At low stresses, kink pairs tend to ''stick'' only when nucleated near a surface. (a) Single kink annihilates with its image. (b) Mobile kink remains in bulk, free to move.

faces also decrease the velocity in that the finite size of the dislocation places a limit on the number of kink pairs that can be present.[2] In this manner, free surfaces can also be thought of as kink sinks.

At low stresses, kink pairs are very unstable and the source behavior of the surface dominates. The dislocation velocity is closely related to the probability of nucleating a kink pair near the surface, since kink pairs nucleated in the bulk are likely to annihilate in the next kinetic Monte Carlo step. This probability is determined by the ratio of surface nucleation sites to bulk nucleation sites. The ratio decreases as the dislocation length is increased, leading to an overall decrease in dislocation velocity as a function of length.

At high stresses, nucleated kink pairs both at the surface and in the bulk are quite stable. Although nucleation at the surface is still favored, there are many more sites in the bulk, and all kink pairs tend to ''stick.'' Once the kinks are nucleated, they spread along the dislocation under the influence of the applied stress until they reach the surfaces. The sink behavior of the surface now dominates; the length dependence of the velocity here is now a consequence of the finite size of the dislocation. If the dislocation is shorter than the equilibrium kink separation, very few (typically, only one) kink pairs can be present at a time before the kinks move off the surface. As the dislocation length increases, more opportunities for kink pair nucleation arise and the dislocation can thus advance more rapidly.

This tendency of the free surfaces to act as kink sources at low stresses and as kink sinks at high stresses can be modeled by the following equation for slip per unit length:

$$\frac{\partial y}{\partial t} = D\frac{\partial^2 y}{\partial x^2} + \alpha \sum_{n=-\infty}^{\infty} \delta(x - nL) + \beta. \tag{9}$$

Here y represents the slip per unit length of the dislocation, D is a kink diffusion coefficient, and L is the dislocation length. β is related to the nucleation rates in an infinite dislocation, and α is related to the additional contribution to the nucleation rates at the surfaces. The sum is taken to be infinite in order to facilitate solution. One expects $\alpha > 0$ for low stresses and $\alpha < 0$ for high stresses.

Solving Eq. (9) for y yields

$$y(x,t) = \left(\frac{\alpha}{L} + \beta\right) t + \frac{\alpha L}{2\pi^2 D} \times \sum_{m=1}^{\infty} \frac{\cos(2\pi m x/L)(1 - e^{-4D\pi^2 m^2 t/L^2})}{m^2}. \tag{10}$$

The dislocation motion is thus described by a constant velocity term and a term that modifies the shape of the dislocation, causing it to form a bowed structure. The strength of this ''bowing'' depends on both the dislocation length and on α, the additional contribution to dislocation slip at the surface. When $t \to \infty$, the time-dependent contribution of this bowing term disappears and the steady-state dislocation velocity is simply

$$\frac{\partial y}{\partial t} = \frac{\alpha}{L} + \beta, \tag{11}$$

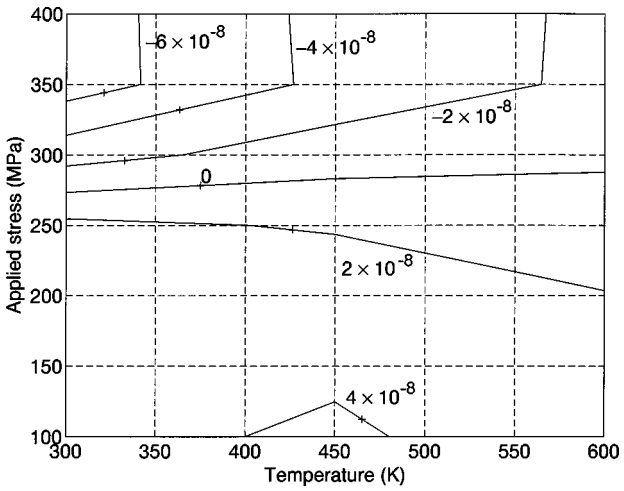

FIG. 4. Contour plot of the characteristic dislocation length α/β, in meters, as a function of applied stress and temperature. The line marked 0 indicates the set of parameters where velocity is independent of dislocation length.

where β now gives the dislocation velocity in the limit of infinite length and α determines the strength of the length dependence. Using Eq. (11), one can fit the velocity data of Fig. 2 to determine α and β as a function of stress and temperature. A contour plot of α/β, where $L^* = |\alpha/\beta|$ is the characteristic length, is shown in Fig. 4. As expected, α is determined to be negative for high stresses and positive for low stresses. The line along which $L^* = 0$ marks the set of stress-temperature pairs where velocity is effectively independent of dislocation length. The values of L^* reported here are short, approximately 400 Å. The velocity of dislocations substantially longer than this will be unaffected by finite size.

Figure 5 displays the steady state velocity of the dislocation as a function of applied stress for three temperatures, using the full simulation including detailed calculation of elastic energies. The velocities are calculated using dislocation lengths of $2000b$. For $T = 450$ K and $T = 600$ K, this is well beyond the region of strong length dependence and the velocities can be considered to be the same as those in the

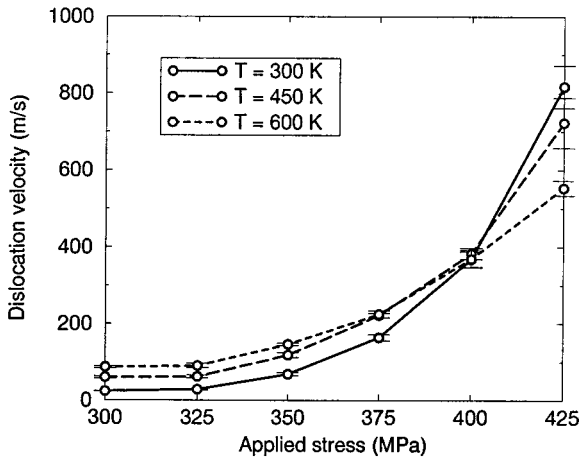

FIG. 5. Dislocation velocity as a function of applied stress for three temperatures. $L = 2000b$ and $\omega_0 = 1.2 \times 10^{12}$ sec^{-1}.

infinite-length limit. For $T=300$ K, this dislocation length is still in the regime where there is significant length dependence. (Note in Fig. 4 that the characteristic length L^* is somewhat higher for $T=300$ K in the stresses of interest.) Thus the velocities are slightly lower than those in the infinite-length limit, and close examination of Fig. 5 reveals that the $T=300$ K curve crosses the other two curves at a higher stress than they cross each other. Although it is impractical to generate the entire $T=300$ K curve with a sufficiently long dislocation due to the computational time needed for such a calculation, it is found by calculating the velocities at the two points $\sigma=375$ MPa and $\sigma=400$ MPa that the $T=300$ K curve will cross the others at the same point in the infinite-length limit. The stress at which this point occurs, ~ 385 MPa, corresponds to the zero-temperature yield stress for a dislocation of infinite length, as is now discussed.

The crossing of the curves at high stress can be understood as follows. The six processes that govern the motion of the dislocation are kink pair nucleation with (i.e., in the direction favored by) or against an applied stress, kink pair annihilation with or against the stress, and lateral kink motion with or against the stress. One may suppose that the velocity of the dislocation is primarily determined by the complementary processes of kink pair nucleation with the stress and kink pair annihilation against the stress. This is not an unreasonable assumption, since kink pair nucleation against the stress occurs rarely and lateral kink motion can occur only after kinks have been nucleated. To explore the relative importance of these two primary processes, the energy barrier associated with each process was plotted as a function of stress, assuming an isolated kink pair in the middle of an otherwise flat dislocation. Since the energy barrier for kink pair nucleation with the stress decreases with increasing stress and the energy barrier for kink pair annihilation against the stress increases with increasing stress, the curves must eventually cross, and do so around 410 MPa. (This does not correspond exactly to the crossing point $\sigma=385$ MPa observed in Fig. 5, since this simple analysis does not take into account the influence of the configuration-dependent long-ranged elastic fields as well as the other processes that affect the motion of the dislocation.) The ratio of the two rates, assumed to be related to the velocity, is given by

$$R_{\mathrm{nuc}}/R_{\mathrm{ann}}=\exp[-(E_{\mathrm{nuc}}-E_{\mathrm{ann}})/kT], \tag{12}$$

where E_{nuc} and E_{ann} are the energy barriers associated with kink pair nucleation and annihilation, respectively. At low stresses, $E_{\mathrm{nuc}}>E_{\mathrm{ann}}$ and the exponent in Eq. (12) is negative; as T increases, the ratio of the rates (and thus the dislocation velocity) also increases. This produces the expected behavior. However, at high stresses, $E_{\mathrm{nuc}}<E_{\mathrm{ann}}$ and the exponent in Eq. (12) is positive, indicating that it is actually energetically favorable to nucleate double kinks. Therefore, as T increases, the exponent approaches zero and the velocity actually decreases.

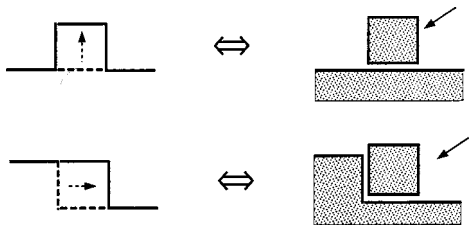

FIG. 6. Analogy between dislocation motion and thin film growth on a 1D substrate. Double-kink nucleation or annihilation corresponds to adatom deposition or evaporation on the flat substrate, and lateral kink motion corresponds to addition or removal of an atom at a ledge.

IV. DYNAMIC SCALING OF DISLOCATION WIDTH

A. Observation of kinetic roughening

As a way of characterizing the dynamics of the dislocation moving through the corrugated Peierls potential, it is insightful to consider the following analogy with the growth of thin films on a one-dimensional substrate:[2] Double-kink nucleation or annihilation corresponds to adatom deposition or evaporation on the flat substrate, and kink motion corresponds to addition or removal of an atom at a ledge (see Fig. 6). In crystal growth models, surfaces typically display dynamic scaling behavior (for a nice review, see Ref. 16). One commonly studied aspect of this behavior is the dynamic scaling of the interface width, defined as

$$w(L,t)=L^{-1/2}\left\{\sum_{i=1}^{N}[h_i(t)-\overline{h}(t)]^2\right\}^{1/2}, \tag{13}$$

where $h_i(t)$ is the position of screw segment i in the dislocation at time t (analogous to the height of a growing thin film), $\overline{h}(t)$ is the average position of the dislocation at time t, and N is the number of segments (i.e., the length of the dislocation is $L=20bN$).

It is known for simple models of growth that the interface width obeys the dynamic scaling form[17]

$$w(L,t)=L^{\zeta}f(t/L^{z}), \tag{14}$$

where ζ and z are scaling exponents and $f(x)$ is a scaling function. One set of exponents often observed can be determined from the analysis of the Kardar-Parisi-Zhang (KPZ) equation, which appears in one dimension as[18]

$$\frac{\partial h}{\partial t}=\Lambda\frac{\partial^2 h}{\partial x^2}+\lambda\left|\frac{\partial h}{\partial x}\right|^2+\eta(x,t)\ . \tag{15}$$

Here h is the displacement (in the slip plane) of the dislocation at position x, Λ represents the strength of the line tension, and $\eta(x,t)$ is an uncorrelated white noise. For $\lambda\neq 0$, one obtains $\zeta=1/2$ and $z=3/2$.[16–18] For $\lambda=0$, the KPZ equation reduces to the Edwards-Wilkinson equation, for which $\zeta=1/2$ and $z=2$.

Figure 7 contains scaled plots of dislocation width vs. time, averaged over at least 200 trials to reduce the effect of statistical noise. (Unscaled data are shown in the inset.) By eye, best collapse of the data was achieved with the exponents $\zeta=0.53$ and $z=1.55$, which are very close to the exponents predicted by the KPZ equation for the general case

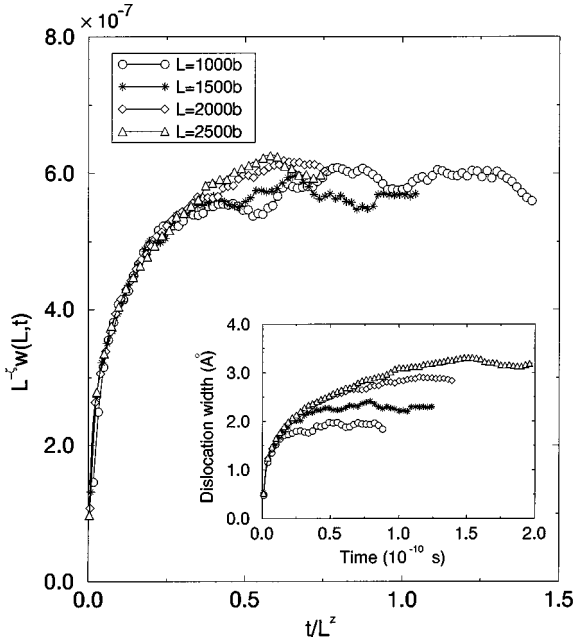

FIG. 7. Dislocation width vs time for four dislocation lengths, scaled according to Eq. (13) using exponents of $\zeta=0.53, z=1.55$ (unscaled data are shown in the inset). Data are for an applied stress of 300 MPa and temperature 450 K.

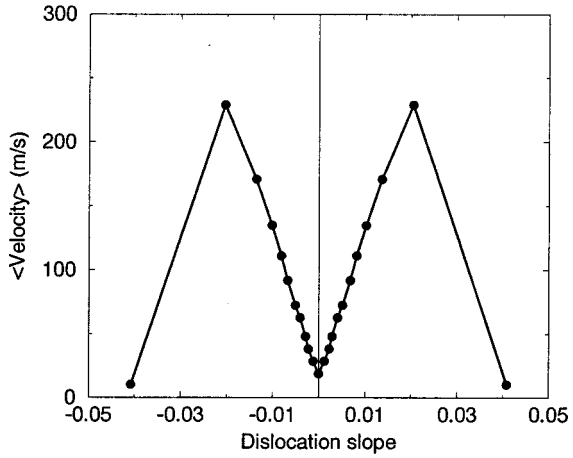

FIG. 8. Expectation value of the dislocation velocity for a perfectly ordered sloped dislocation as a function of the slope. This dependence suggests that the λ of Eq. (15) is nonzero. Data are for a dislocation of length 2000b, applied stress of 300 MPa, temperature 450 K.

$\lambda \neq 0$. This suggests that the dislocations do display kinetic roughening, and that the exponents governing this scaling are those appropriate to the KPZ model of thin film growth.

It is noted that in order to observe this scaling in the simulations, one must be in the limit in which the bowing of the dislocation predicted by Eq. (10) is much less than the width predicted by Eq. (13). The bowing predicted from Eq. (10) scales with α, and hence the ideal parameters for the study of this behavior are those along the contour $\alpha/\beta=0$ in Fig. 4. In practice, however, producing Fig. 4 for the full simulations (including all elastic interactions), and thus determining these parameters accurately, is difficult. It is also noted that the dislocation widths estimated from the simulation are quite narrow, and probably cannot be observed through experiment.

B. Analysis of scaling results

In Eq. (15), $\lambda \neq 0$ corresponds to a dependence of the dislocation velocity on the local slope. Given that the dislocation width scales according to the KPZ exponents, one should expect to be able to observe this dependence. Figure 8 shows the expectation value of the dislocation velocity for perfectly ordered, sloped configurations as a function of the slope. The slope dependence is apparent, and is consistent with the observation of KPZ scaling.

With perfectly ordered configurations, this dependence of the velocity on the slope of the dislocation can easily be seen to arise from the difference between the rates of double-kink nucleation and lateral kink motion. For a perfectly flat dislocation, no kinks are present and the expectation value of the velocity thus depends only on the rate of kink-pair formation. For a maximally sloped dislocation, there exist no sites for kink-pair formation and the velocity depends only on the rate of lateral kink motion. A dislocation with an intermediate slope will have its velocity determined by both rates, weighted according to the number of sites for each type of event. Since rates for double-kink nucleation and lateral kink motion are expected to be different in general, one expects always to observe KPZ scaling of the dislocation width within this model, regardless of the choice of parameters.

The precise role the solid-on-solid condition plays in the observed kinetic roughening is not clear. Kinks of like sign do approach within the minimum distance. One might expect the imposed condition, which prevents the formation of extended edge segments and ''overhangs,'' to exert an overall smoothing influence on the dislocation width. If so, then the kinetic roughening observed here represents a ''lower bound'' on the effects of the nonlinearity on the dislocation dynamics. Removal of the solid-on-solid constraint may lead to more dramatic changes in the manner in which the dislocation propagates through the Peierls valleys. The implication is that under conditions of high stress, the nonlinearities governing dislocation motion cannot be neglected.

V. CONCLUSIONS

In conclusion, a kinetic Monte Carlo simulation of dislocation dynamics has been introduced and studied. The model represents a simple version of a dislocation moving through a deep Peierls potential and a deep secondary Peierls potential as well. The impact of stress, temperature, and finite size on the dislocation velocity and structure are investigated. The simulations confine the dislocation to move on a lattice, and the double-kink nucleation and annihilation rates, as well as the kink migration rates, are calculated reflecting both the effects of the elastic interactions and the presence of surfaces.

The effects of finite size on the velocity of the dislocation are examined, and it is found that dislocation velocity decreases with length at low stresses and increases with length for high stresses. This dependence is a result of the stability of nucleated kink pairs as a function of stress and temperature. At low stresses where kink pairs are unstable, the sur-

faces act as kink sources and the velocity is related to the ratio of surface sites to bulk sites, which decreases with length. At high stresses where kink pairs are stable, the number of kink pairs is limited primarily by the length of the dislocation; thus, the velocity is observed to increase with length.

The dislocation velocity is observed to increase with applied stress. The effects of temperature on the dislocation velocity, however, are somewhat unexpected. At low stresses, thermal fluctuations enhance the mobility of the dislocation, and the velocity of the dislocation increases with increasing temperature. At high stresses, the nucleation of double kinks is favored, and thermal fluctuations serve to decrease the double kink nucleation rate, hence slowing the dislocation. It is argued that the stress at which the velocity is temperature independent, for a dislocation of infinite length, corresponds to the zero-temperature yield stress.

Through an analogy with models of thin film growth, the dislocation width is shown to exhibit dynamic scaling governed by exponents predicted by the Kardar-Parisi-Zhang equation. This result corresponds to a dependence of the dislocation velocity on the local slope of the dislocation. This dependence can be explicitly observed, and arises from the difference in the rates of the two possible types of events, kink-pair formation or annihilation and lateral motion of a single kink. Since these rates are expected to be different in general, the model suggests that KPZ scaling will be observed for dislocations under applied stresses and temperatures in which finite-size effects are insignificant.

ACKNOWLEDGMENTS

The authors acknowledge J. Hirth for insightful conversations. Computer time provided by the National Energy Supercomputer Research Center is gratefully acknowledged. This work was supported by the Department of Energy, Office of Basic Energy Sciences, Division of Materials Science under Contract No. DE-AC03-76SF00098.

[1] G. H. Campbell, S. M. Foiles, H. Huang, D. A. Hughes, W. E. King, D. H. Lasilla, D. J. Nikkel, T. D. de la Rubia, J. Y. Shu, and V. P. Smyshlyaev, Mater. Sci. Eng. A **251**, 1 (1998).
[2] J. P. Hirth and J. Lothe, *Theory of Dislocations*, 2nd ed. (Krieger Publishing Company, Malabar, Florida, 1992).
[3] M. Tang, L. P. Kubin, and G. R. Canova (unpublished).
[4] A. Seeger and P. Schiller, in *Physical Acoustics*, edited by W. P. Mason (Academic, New York, 1966), Vol. 3A.
[5] P. A. Maksym, Semicond. Sci. Technol. **3**, 594 (1988).
[6] T. Suzuki, H. Koizumi, and H. O. K. Kirchner, Acta Metall. Mater. **43**, 2177 (1995).
[7] S. Nemat-Nasser and J. B. Isaacs, Acta Mater. **45**, 907 (1997).
[8] J. W. Christian, Metall. Trans. A **14A**, 1237 (1983).
[9] Y. Maurissen and L. Capella, Philos. Mag. **29**, 1227 (1974).
[10] Y. Maurissen and L. Capella, Philos. Mag. **30**, 679 (1974).
[11] J. Bennetto, R. W. Nunes, and D. Vanderbilt, Phys. Rev. Lett. **79**, 245 (1997).
[12] W. Xu and J. A. Moriarty, Comput. Mater. Sci. **9**, 348 (1998).
[13] Y. M. Huang, J. C. H. Spence, and O. F. Sankey, Phys. Rev. Lett. **74**, 3392 (1995).
[14] V. V. Bulatov, S. Yip, and A. S. Argon, Philos. Mag. A **72**, 453 (1995).
[15] H. R. Kolar, J. C. H. Spence, and H. Alexander, Phys. Rev. Lett. **77**, 4031 (1996).
[16] J. Krug and H. Spohn, in *Solids Far From Equilibrium*, edited by C. Godrèche (Cambridge University Press, Cambridge, 1992).
[17] F. Family and T. Vicsek, J. Phys. A **18**, 75 (1985).
[18] M. Kardar, G. Parisi, and Y. C. Zhang, Phys. Rev. Lett. **56**, 889 (1986).